PORE NETWORK SIMULATION OF LOW-FIELD NMR RELAXOMETRY UNDER CONDITIONS OF DRAINAGE AND IMBIBITION: EFFECTS OF PORE STRUCTURE AND SATURATION HISTORY

D. Chang and M.A. Ioannidis
Porous Media Research Institute
Department of Chemical Engineering
University of Waterloo, CANADA

ABSTRACT

Nuclear magnetic resonance (NMR) relaxometry tests, carried out on partially saturated porous media, convey information on the distribution of fluids within the pore space. Proper interpretation of this information requires a means to isolate the effects of pore structure (pore and throat shape and size distributions, spatial correlations, etc.) wettability and saturation history. A pore network simulator of NMR relaxation that can clarify the effect of these factors on observed T2 distributions is developed in this work. The pore network model can be calibrated with pore structure parameters (pore volume and throat size distributions, pore connectivity) determined from analysis of stochastic 3D replicas of the pore space generated from thin-section image information. The presence of irregular and, possibly, fractal pore surfaces is accounted for through a "late pore filling" model calibrated to match mercury porosimetry data. The network model is then used to simulate the water distribution and proton magnetization decay under conditions of drainage and imbibition. The results obtained reveal: (a) conditions under which diffusive coupling between pores has a significant effect on the decay spectra, (b) contributions to the magnetization decay spectra from water trapped at the irregular pore surfaces, and (c) contributions to the magnetization decay spectra from (i) water in large pores which are inaccessible by the non-wetting phase during drainage and (ii) water in pores containing oil trapped during imbibition.

INTRODUCTION

With the increasing use of NMR techniques in the field and laboratory, there is a need to clarify how the NMR response of partially saturated reservoir rock depends on pore structure parameters, wettability and displacement history. Pore network simulation has been used extensively in the past to study the relationship of the aforementioned factors on capillary pressure, electrical resistivity and relative permeability. In recent years, pore network simulation has been endowed with predictive power, as a result of advances in (a) 3D stochastic reconstruction from thin-section image statistical information (Ioannidis *et al.*, 1999; Liang *et al.*, 2000; Bekri *et al.*, 2000) and (b) grain deposition/diagenesis modeling (Bakke and Øren, 1997). If pore network models are to be further developed as tools for petrophysical evaluation, then their extension to include predictions of the NMR response of reservoir rock should be considered. This task was recently undertaken by Chang *et al.* (2000) and is further pursued in the present contribution.

back to contents

In a NMR measurement, hydrogen atoms on water molecules probe the pore space by diffusive motion. The magnetic moment carried by these atoms relaxes due to dipolar interactions with other molecules and with the fluid-solid interface. For a single pore in the fast diffusion limit, the surface relaxation rate is slow compared to the rate of magnetization equilibration by diffusive motion (Brownstein and Tarr, 1979). Consequently, magnetization is approximately uniform across the pore and decays with a characteristic time T_2 that is inversely proportional to the pore's surface area-to-volume ratio:

$$\frac{1}{T_2} = \rho \frac{A}{V} \tag{1}$$

The proportionality constant ρ is known as the surface relaxivity and knowledge of its value allows one to convert a rate of surface relaxation to a characteristic pore size R_P (*e.g.*, $A/V = 3/R_P$ for spherical pores). The time evolution of proton magnetization in sedimentary rocks is usually characterized by a spectrum of decay rates (Kenyon, 1997), a fact used to estimate the distribution of pore volume by pore size. Such estimates are invariably made under the assumption that, although in the fast diffusion limit, individual pores are uncoupled from their neighbors. The effect of this assumption has been theoretically investigated by McCall *et al.* (1991). These authors studied network models in which the sizes of pores were broadly distributed, but the pore throat cross-sectional areas and inter-pore diffusion lengths were assumed constant. Such models are not representative of the pore structure of reservoir rocks, in which pore throat sizes and inter-pore lengths are also broadly distributed. McCall *et al.* (1991) suggested that in a system with a broad distribution of pore sizes, in the range typically found in sandstones, pore coupling should be marginally significant. This implies that the spectrum of decay rates obtained by multi-exponential decomposition of total magnetization measurements should reflect the volume density of pore sizes reasonably well. This is conclusion is not generally true, especially at conditions of partial saturation (Chang *et al.*, 2000).

A primary drainage capillary pressure curve provides the distribution of pore volume accessible to a non-wetting phase by capillary pressure. The latter is related to the size of pore throats that are accessible by a non-wetting phase during drainage through the Laplace equation:

$$P_c = \frac{\sigma f(\theta)}{R_t} \tag{2}$$

where R_t is a characteristic pore throat size and $f(\theta)$ is a function of the receding contact angle that depends on the geometry of the pore throat cross-section (*e.g.*, $f(\theta) = 2\cos\theta$ for cylindrical pore throats). Under imbibition conditions Eq. (2) also governs the piston-type retraction of non-wetting phase from pore bodies and pore throats. Under such conditions, the angle θ is the advancing contact angle. The difference between receding and advancing contact angles (contact angle hysteresis) is a cause of hysteresis between the drainage and imbibition capillary pressure curves. Quasistatic imbibition is controlled by the interplay between two main types of capillary instability: piston-type retraction of fluid interfaces from pore bodies and pore throats and snap-off of non-wetting phase threads in pore throats (Ioannidis and Chatzis, 1993a). The collective outcome of these pore-level phenomena is the establishment of a residual non-wetting phase saturation, the magnitude of which is determined by the geometry and connectivity of the pore space and by wettability.

The mercury-air drainage and imbibition curves are a strong signature of the geometry, connectivity and spatial arrangement of pore bodies and pore throats within a rock sample. Their prediction is, therefore, a rigorous test on a network model's ability to represent the porous microstructure of real rock. The task of developing pore network models which honor experimental mercury porosimetry data is, however, highly nontrivial (Tsakiroglou and Payatakes, 2000). A main difficulty arises from the fact that real pores have an irregular, rough and often fractal geometry. When a non-wetting fluid first invades a pore in real rock, the amount of wetting phase that remains within this pore is considerably larger than would be predicted by assuming that the pore has a regular, albeit angular, cross-section (Ioannidis and Chatzis, 1993b). Neglect of this fact imparts considerable uncertainty on network model calculations, certainly regarding volumetric calculations and possibly regarding calculations of electrical resistivity and relative permeability.

In this work we propose a simple "late pore filling" model to account for the rough or fractal pore geometry. Use of this model permits a description of proton magnetization evolution at conditions of partial saturation in a manner that is consistent with image analysis and mercury porosimetry data. This model is the new feature in a mixed-percolation algorithm that is employed to simulate primary drainage and imbibition in model pore networks. At each level of wetting phase saturation along the drainage and imbibition path, the associated NMR problem is solved using a matrix diagonalization method (Chang *et al*., 2000; McCall *et al.*, 1991). Results are presented which illustrate the effects of pore structure and saturation history on magnetization evolution.

METHODOLOGY

Construction of model pore networks

The pore structure model used is similar to the one used by Ioannidis and Chatzis (1993b) to simulate the permeability, formation factor and drainage capillary pressure curves of several sandstones. It is a simple cubic network of pores and throats of square cross-section (Fig. 1). Pore body sizes are randomly assigned to the sites of the network, whereas pore throat sizes are correlated to the size of the smaller of the two pores each throat connects. Pore body and pore throat sizes are assumed to follow respective Weibull distribution functions (Shapiro and Gross, 1981):

$$f_i(R) = \left(\frac{ß}{a}\right)\cdot\left(\frac{R - R_{min}}{a}\right)^{ß-1}\cdot\exp\left[-\left(\frac{R - R_{min}}{a}\right)^{ß}\right] \qquad \begin{array}{l} i = p,b \\ p = pores \\ t = throats \end{array} \qquad (3)$$

where a, b are parameters of the distributions and R_{min} is a minimum pore body or pore throat size. The inter-pore lengths are also distributed in the network according to a Weibull distribution and are positively correlated to the size of adjoining pores. These lengths are only used to estimate the resistance to diffusion and fluid flow between adjacent pores; all pore volume is assigned to the pore bodies. The network model thus constructed is a realistic approximation of pore networks in 3D stochastically reconstructed porous media (Liang *et al*., 2000; Ioannidis and Chatzis, 2000). Network models containing 15^3 pore bodies are used throughout this work. All results reported are averages over 10 realizations.

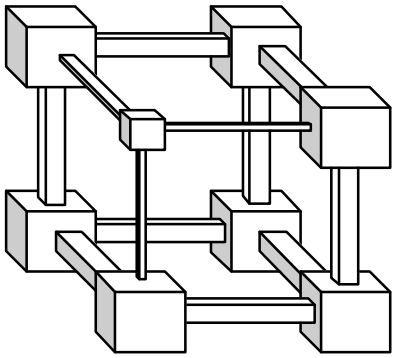

Figure 1: Schematic representation of the geometry of the pore network model.

Simulation of magnetization evolution in model pore networks

A balance of magnetization M_i may be written for each pore i in the network. The net rate of magnetization decay in each pore is determined by magnetization relaxation in the vicinity of the fluid-matrix interface and by diffusion to and from neighboring pores:

$$\frac{dM_i}{dt} = -\rho A_i \frac{M_i}{V_i} + D \sum_j^{NN} \frac{S_{ij}}{L_{ij}} \left(\frac{M_j}{V_j} - \frac{M_i}{V_i} \right) \tag{4}$$

where A_i, V_i are the surface area and volume of pore i, respectively, D is the diffusion coefficient of water and S_{ij}, L_{ij} are the cross-sectional area and length of connecting pore throats. In dimensionless form, Eq. (4) may be written as follows:

$$\frac{dM_i}{dt} = -\rho_\rho r_i M_i + \rho_c \sum_j^{NN} \frac{s_{ij}}{l_{ij}} \left(\frac{M_j}{v_j} - \frac{M_i}{v_i} \right) \tag{5}$$

In writing Eq. (5) the following definitions are used:

$$w_r = r \frac{\overline{A}}{\overline{V}} = \frac{1}{t_o} \qquad w_c = \frac{D\overline{S}}{\overline{V}\,\overline{L}}$$

$$s_{ij} = \frac{S_{ij}}{\overline{S}} \qquad l_{ij} = \frac{L_{ij}}{\overline{L}} \tag{6}$$

$$v_{ij} = \frac{V_{ij}}{\overline{V}} \qquad r_i = \frac{A_i}{V_i} \frac{\overline{V}}{\overline{A}}$$

In the equations above, overbars indicate average quantities. The parameters w_r and w_c represent a characteristic rate of relaxation at the fluid-solid interface and a characteristic rate of molecular diffusion between pores, respectively. Application of Eq. (5) to each pore yields an initial-value, linear ordinary differential equation problem, which is most efficiently solved by matrix diagonalization. The solution provides the volume-weighted distribution $n(l)$ of decay rates l, hereafter referred to as the spectrum of decay rates, where each l is an eigenvalue of the problem. In the absence of coupling between pores,

$l_i = rA_i/V_i$ and the spectrum $n(l)$ exactly corresponds to the distribution of pore volume by inverse pore size.

Simulation of primary drainage and primary imbibition

Simulation of primary drainage is carried out using a bond-correlated site percolation algorithm described in detail by Ioannidis and Chatzis (1993b). The capillary pressure for piston-type non-wetting phase invasion into a pore throat is calculated from Eq. (2). For pore throats of rectangular cross-section the function $f(q)$ is (Legait, 1983):

$$f(\theta) = \frac{\theta + \cos^2\theta - \pi/4 - \sin\theta\cos\theta}{\cos\theta - \sqrt{\pi/4 - \theta + \sin\theta\cos\theta}} \tag{7}$$

where q is the receding contact angle. (*i.e.*, $f(q) = 1.5274$ when $q = 40^o$). The capillary pressure for piston-type retraction of non-wetting phase from a pore body is also calculated by equation (2), where the advancing contact angle is used to calculate $f(q)$. The critical pressure ratio (CPR) is defined as the ratio of capillary pressure for piston-type retraction from a pore throat to the critical capillary pressure for snap-off (Li and Wardlaw, 1986) and is a function of pore throat geometry and contact angle. Knowledge of this parameter enables the calculation of the capillary pressure for snap-off as:

$$P_{c,snap-off} = \frac{s\,f(\theta_a)/R_t}{CPR} \tag{8}$$

A mixed percolation algorithm is used to simulate quasistatic imbibition. This algorithm has been detailed elsewhere (Ioannidis and Chatzis, 1993a).

Late pore filling model

We propose that upon invasion of the non-wetting fluid into each individual pore at capillary pressure P_c^*, a fraction S_w^* of the volume of the pore is occupied by the wetting fluid. The fraction of the volume of the pore that contains wetting fluid at capillary pressure $P_c > P_c^*$, is assumed to vary according to the following expression (Brooks and Corey, 1964):

$$\frac{S_w}{S_w^*} = \left(\frac{P_c^*}{P_c}\right)^{\eta} \tag{9}$$

The fraction S_w^* and late pore filling exponent h are model parameters. For $0 < h < 1$ late pore filling corresponds to filling of a surface fractal with dimension $2 < D_s < 3$, whereas for $h > 1$ the pore behaves as a rough, but not fractal, object. The parameter S_w^* may be identified with the fraction of total pore volume contributed by length scales not explicitly represented in network models. The value of P_c^* is different for each pore and depends on the pore throat size and pore accessibility. During primary imbibition, and for as long as piston-type retraction or disconnection of the non-wetting fluid in a pore has not taken place, the wetting fluid content of a pore increases according to Eq. (9).

RESULTS AND DISCUSSION

Simulation parameters

Pore structure parameters used in the simulations are typical of sandstone. Simulation parameters are listed in Table 1, whereas the pore size, throat size, and inter-pore length size distributions are depicted in Figure 2. Surface relaxivity values ranging from 5 μm/s to greater than 100 μm/s have been reported for sandstones (Howard *et al.*, 1993; Slijkerman and Hofman, 1998; Roberts *et al.*, 1995; Kleinberg, 1996). A surface relaxivity value of 100 μm/s is used in all computations reported here. A critical pressure ratio (CPR) equal to 6 was used in all simulations. Although the value of CPR can be estimated from knowledge of contact angle and pore throat geometry (Ioannidis and Chatzis, 1993), CPR is treated as an adjustable parameter in our simulations.

Capillary pressure curves including late pore filling

Figure 3 illustrates the effect of parameter S_w^* on the simulated drainage and imbibition capillary pressure curves for a value of h = 1.5 (rough, but not fractal pores). Results from 10 different realizations are plotted to illustrate the magnitude of variability. As the amount of wetting fluid remaining in pores upon penetration by the non-wetting fluid (S_w^*) increases, the increase of S_{nw} with increasing capillary pressure becomes much more

Table 1 : Simulation parameters.

Parameter	*value*
Mean of PSD (μm)	15.6
Standard deviation of PSD (μm)	5.6
Minimum pore size (μm)	1
Mean of TSD (μm)	5.6
Standard deviation of TSD (μm)	2.8
Minimum throat size (μm)	0.1
Mean of LSD (μm)	9.45
Standard deviation of LSD (μm)	5.67
Minimum diffusion length (μm)	1
Water diffusivity ($\mu m^2/s$)	2500
Surface relaxivity, r (μm/s)	100
Critical pressure ratio	6
Receding contact angle	40^o
Advancing contact angle	60^o
S_w^*	0.06 & 0.24
h	1.5 & 0.5

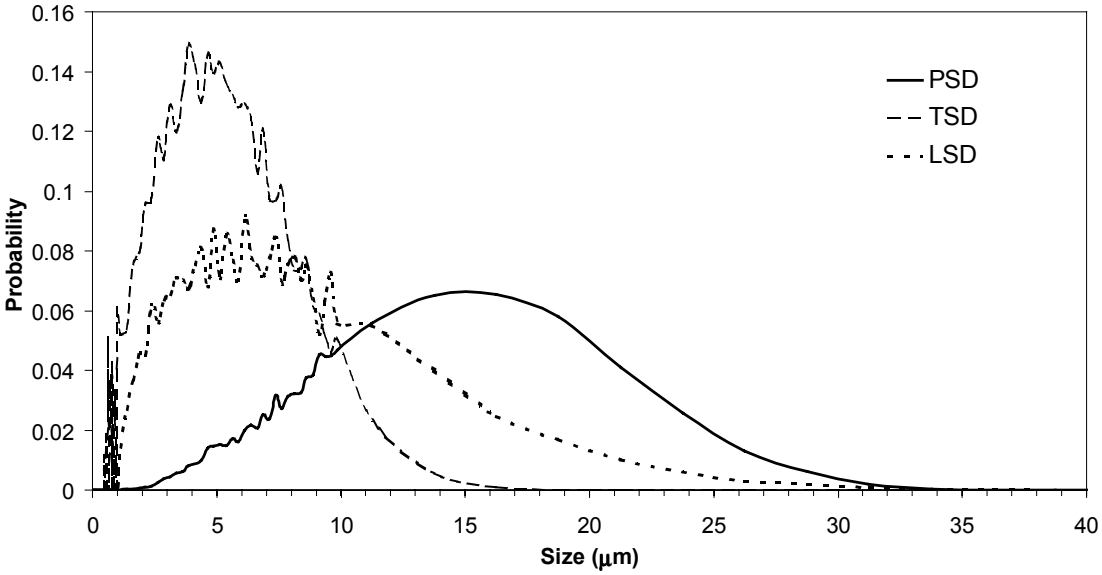

Figure 2: Pore size, throat size and inter-pore length distributions used in simulations.

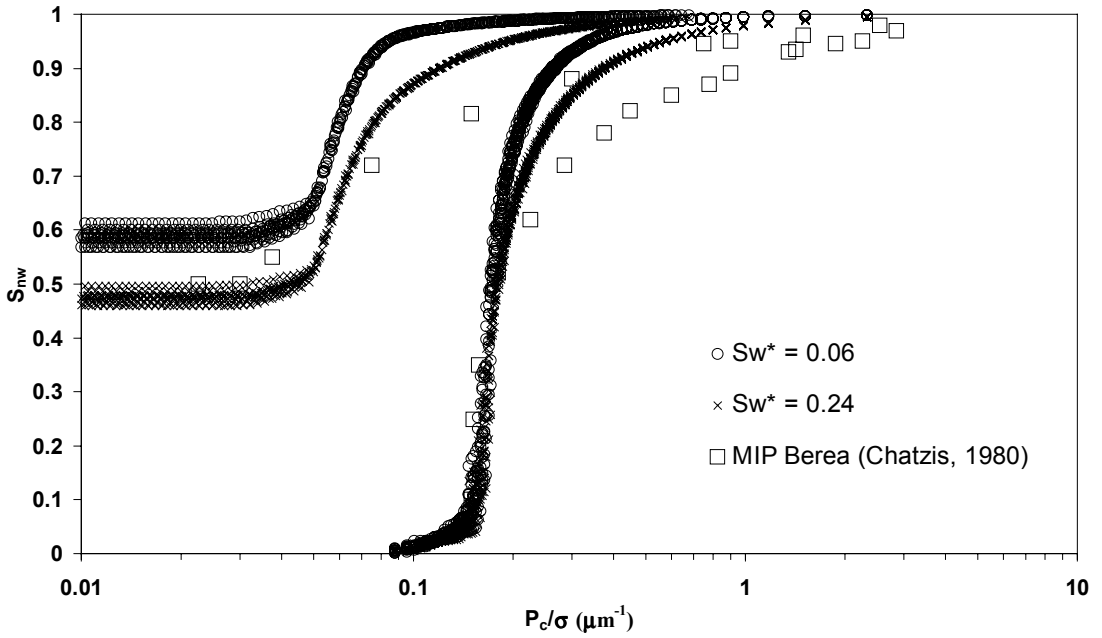

Figure 3: Effect of parameter S_w^* on simulated capillary pressure curves (η = 1.5).

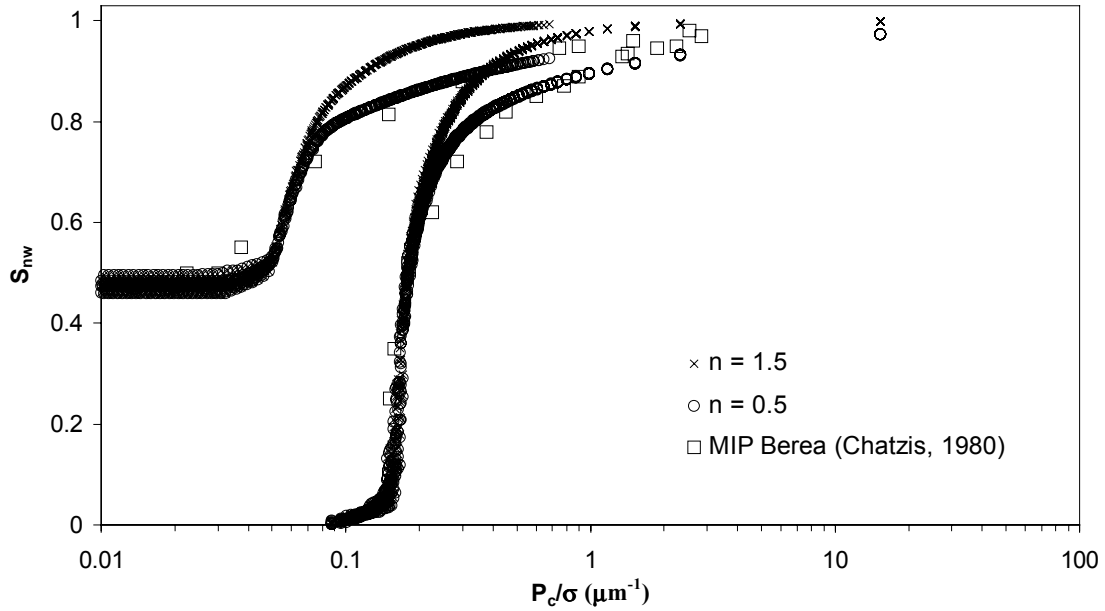

Figure 4: Effect of parameter η on simulated capillary pressure curves ($S_w^* = 0.24$).

gradual. During imbibition, a greater amount of non-wetting fluid is displaced before a large number of piston-type retraction events take place. The main leg of the imbibition curve is not affected, but the residual non-wetting phase saturation is considerably reduced. The effect of parameter η is illustrated in Figure 4. As can be seen, changing η from 1.5 (non-fractal pore geometry) to 0.5 (fractal pore geometry) results in even more gradual drainage and imbibition curves. Changing η has no effect on the residual non-wetting phase saturation. The results, which are clearly representative of experimental mercury porosimetry curves of sandstones, demonstrate the flexibility of the late pore filling model. This model provides a means of capturing pore structure effects from unresolved length scales (*e.g.,* microporosity). Its application in the network modeling of electrical resistivity of partially saturated porous media will be addressed in a forthcoming communication.

Effect of saturation history on the NMR response

The spectra of magnetization decay rates for given water content during drainage and imbibition are compared in Figure 5. These results were obtained using $S_w^* = 0.24$ and $\eta = 1.5$ and may be explained as follows. During drainage, the larger pores are preferentially filled with nonwetting fluid. Note that we do not consider bulk relaxation effects and therefore no oil signal is reported in the simulations. The wetting fluid in the invaded pores continues to be in contact with the entire surface of the pore, but its volumetric content decreases. This results in the gradual disappearance of the slower decay rates (long T_2 values) as the effective surface to volume ratio of the invaded pores increases (Fig. 5(a)). The remaining slow decay rates present in the spectrum belong to larger pores that are inaccessible by the non-wetting fluid.

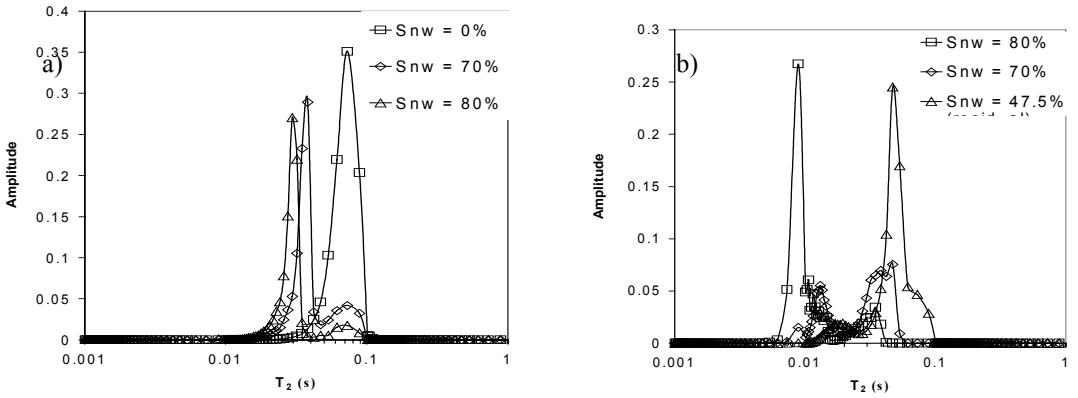

Figure 5: Spectra of proton magnetization decay rates during (a) drainage and (b) imbibition.

During imbibition, the smaller pores are preferentially invaded by the wetting fluid, resulting in gradual disappearance of the faster decay rates (short T_2 values), as shown in Figure 5(b). The spectrum gradually shifts to slower rates as an increasingly greater amount of water exists in larger pores. As the nonwetting phase saturation decreases, the spectrum of decay rates shown in Figure 5(a) for S_{nw} = 0% is only partly recovered due to the presence of residual nonwetting phase saturation. This is more clearly shown in Figure 6 (b). Note the presence of a second peak in the spectrum at conditions of residual nonwetting phase saturation. Pores containing trapped non-wetting phase also contain a significant amount of water whose characteristic relaxation rate is faster (short T_2 values) than any of the rates appearing in the spectrum from the water-saturated medium. This is because the water in pores containing trapped oil is in contact with the entire pore surface. Figure 6(a) compares NMR relaxation rate spectra at the same saturation (S_{nw} = 0.7) for drainage and imbibition. These spectra reflect the markedly different distribution of water in each case. Clearly, interpretation of these spectra in terms of pore structure parameters cannot be made in the absence of knowledge regarding the saturation history. During drainage, pores not accessible to non-wetting phase contribute to the slow-rate end of the spectrum. During imbibition, many of these pores contain trapped oil resulting in the appearance of a second peak corresponding to fast relaxation rates in the spectrum.

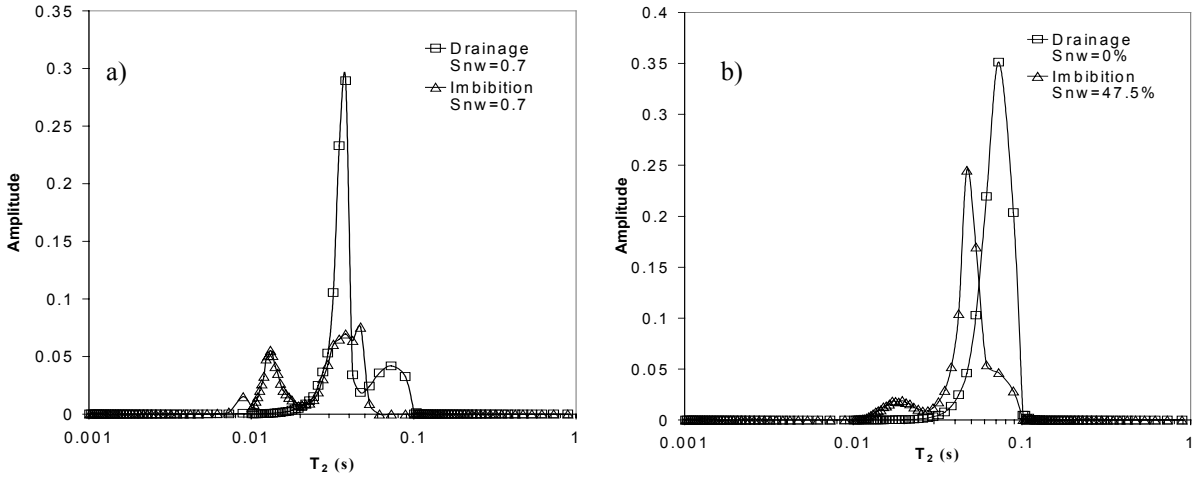

Figure 6: Effects of saturation history on the NMR spectra.

CONCLUSIONS

A pore network model capable of simulating the NMR response of porous rock under conditions of drainage and imbibition was developed. This model takes into account, in a physically based manner, drainage and imbibition associated with pore space features not explicitly accounted for in the pore and throat size distributions. As a result the model is capable of simulating experimentally measured drainage and imbibition capillary pressure curves. Simulations of NMR relaxation reveal rich behavior that is explained in terms of the pore scale mechanisms of drainage and imbibition. The model has all the features necessary for establishing quantitative relationships between the NMR response of partially saturated rock and petrophysical properties of paramount importance such as resistivity index and relative permeability.

NOMENCLATURE

T_2 – NMR relaxation time (s)
A_i – Surface area of pore i (μm^2)
V_i – Volume of pore i (μm^3)
S_{ij} – Cross sectional area of throat connecting pores i and j (μm^2)
L_{ij} – Diffusion length between pores i and j (μm)
R_p – Charateristic pore size (μm)
R_t – Characteristic throat size (μm)
R_{min} – Minimum pore or throat size (μm)
D – Diffusion coefficient ($\mu m^2/s$)
M_i – Normalized magnetization of pore i
S_w – Wetting phase saturation
S_w^* – Wetting phase saturation in a single pore at non-wetting phase invasion
P_c – Capillary pressure (Pa)
P_c^* – Capillary pressure for non-wetting phase invasion (Pa)
CPR – Critical Pressure Ratio (scaling factor between piston type withdrawal and snap-off pressures for pore throats)
D_s – Fractal dimensionality of pore space
α – Weibull location/spread parameter
β – Weibull kurtosis/skewness parameter
ρ – Surface relaxivity ($\mu m/s$)
σ – Surface tension (N/m)
ω_ρ – Characteristic rate of relaxation at the fluid-solid interface (1/s)
ω_c – Characteristic rate of molecular diffusion between pores (1/s)
λ – Relaxation rate (1/s)
η – Late pore filling exponent

REFERENCES

Bakke, S. and Øren, P.E., "3D Pore-scale modeling of sandstones and flow simulations in the pore networks", SPE Journal, (1997) 2, 136-149.

Bekri, S., Xu, K., Yousefian, F., Adler, P.M., Thovert, J.-F., Muller, J., Iden, K., Psyllos, A., Stubos, A.K. and Ioannidis, M.A., "Pore geometry and transport properties in North Sea chalk", Journal of Petroleum Science & Engineering, (2000) 25, 107-134.

Brooks, R.H. and Corey, A.T., "Hydraulic properties of porous media", Colorado State University Hydrology Paper 3, (1964), 27.

Brownstein, K.R. and Tarr, C.E., "Importance of classical diffusion in NMR studies of water in biological cells", Physical Review A, (1979) 19, 2446-2453.

Chang, D., Ioannidis, M.A. and Chatzis, I., "Relationships between non-wetting phase invasion and magnetization evolution in connected pore systems as revealed by network simulation", *Oct 18-22, 2000*, *Abu Dhabi, United Arab Emirates,* Annual Symposium of the Society of Core Analysts.

Chatzis, I. A Network Approach to Analyze and Model Capillary and Transport Phenomena in Porous Media, Ph.D Thesis, University of Waterloo, 1980.

Howard, J.J., Kenyon, W.E. and Straley, C., "Proton magnetic resonance and pore size variations in reservoir sandstones", SPE Formation Evaluation, (1993) September, 194-200.

Ioannidis, M.A. and Chatzis, I., "A mixed-percolation model of capillary hysteresis and entrapment in mercury porosimetry", Journal of Colloid and Interface Science, (1993a) 161, 278-291.

Ioannidis, M.A. and Chatzis, I., "Network modeling of pore structure and transport properties of porous media", Chemical Engineering Science, (1993b) 48, no. 5, 951-972.

Ioannidis, M.A., Chatzis, I. and Kwiecien, M.J., "Computer enhanced core analysis for petrophysical properties", Journal of Canadian Petroleum Technology, (1999) 38, 18-25.

Ioannidis, M.A. and Chatzis, I., "On the geometry and topology of 3D stochastic porous media", Journal of Colloid and Interface Science, (2000) 229, 323-334.

Kenyon, W.E., "Petrophysical principles of applications of NMR logging", The Log Analyst, (1997) 38, no. 2, 21-43.

Kleinberg, R.L., "Utility of NMR T_2 distributions, connection with capillary pressure, clay effect, and determination of the surface relaxivity parameter ρ_2", Magnetic Resonance Imaging, (1996) 14(7/8), 761-767.

Legait, B., "Laminar flow of two phases through a capillary tube with variable square cross-section", Journal of Colloid and Interface Science, (1983) 96, no. 1, 28.

Li, Y. and Wardlaw, N.C., "The influence of wettability and critical pore-throat aspect ratio on snap-off", Journal of Colloid and Interface Science, (1986) 109, 461.

Liang, Z., Ioannidis, M.A. and Chatzis, I., "Permeability and electrical conductivity from 3D stochastic replicas of the microstructure", Chemical Engineering Science, (2000) 55, 5247-5262.

McCall, K.R., Johnson, D.L. and Guyer, R.A., "Magnetization evolution in connected pore systems", Physical Review B, (1991) 44, no. 14, 7344-7355.

Roberts, S.P., McDonald, P.J., and Pritchard, T., "A bulk and spatially resolved NMR relaxation study of sandstone rock plugs", Journal of Magnetic Resonance, (1995) Series A 116, 189-195.

Shapiro, S.S. and Gross, A.J., "Statistical Modeling Techniques", Marcel Dekker, New York, 1981.

Slijkerman, W.F.J., and Hofman, J.P., "Determination of surface relaxivity from NMR diffusion measurements", Magnetic Resonance Imaging, (1998) 16, no. 5/6, 541-544.

Tsakiroglou, C.D. and Payatakes, A.C., "Characterization of the pore structure of reservoir rocks with the aid of serial sectioning analysis, mercury porosimetry and network simulation", Advances in Water Resources, (2000) 23, 773-789.

back to contents